JOURNAL OF VIROLOGY, June 2004, p. 5973–5982 Vol. 78, No. 11
0022-538X/04/$08.00+0 DOI: 10.1128/JVI.78.11.5973–5982.2004

Intracellular Topology and Epitope Shielding of Poliovirus 3A Protein

Sunny S. Choe[1] and Karla Kirkegaard[2]*

Departments of Molecular Pharmacology[1] and Microbiology and Immunology,[2] Stanford University School of Medicine, Stanford, California 94305

Received 26 November 2003/Accepted 24 January 2004

The poliovirus RNA replication complex comprises multiple viral and possibly cellular proteins assembled on the cytoplasmic surface of rearranged intracellular membranes. Viral proteins 3A and 3AB perform several functions during the poliovirus replicative cycle, including significant roles in rearranging membranes, anchoring the viral polymerase to these membranes, inhibiting host protein secretion, and possibly providing the 3B protein primer for RNA synthesis. During poliovirus infection, the immunofluorescence signal of an amino-terminal epitope of 3A-containing proteins is markedly shielded compared to 3A protein expressed in the absence of other poliovirus proteins. This is not due to luminal orientation of all or a subset of the 3A-containing polypeptides, as shown by immunofluorescence following differential permeabilization and proteolysis experiments. Shielding of the 3A epitope is more pronounced in cells infected with wild-type poliovirus than in cells with temperature-sensitive mutant virus that contains a mutation in the 3D polymerase coding region adjacent to the 3AB binding site. Therefore, it is likely that direct binding of the poliovirus RNA-dependent RNA polymerase occludes the amino terminus of 3A-containing polypeptides in the RNA replication complex.

Poliovirus RNA replication occurs on the cytoplasmic surface of membranous vesicles that are derived from the endoplasmic reticulum (ER) and proliferate during viral infection (7, 8, 11, 31, 39, 41, 42, 44, 45). Although all viral proteins are synthesized by cytosolic ribosomes, the viral proteins and nominal precursors that are required for RNA replication (2A, 2B, 2BC, 3A, 3AB, 3CD, and 3D) can be physically localized to these vesicles. Several of these proteins, specifically, 2B, 2C, 3A, and any larger proteins that contain them, target intracellular membranes even when expressed in isolation and are therefore thought to be responsible for the membrane localization of the entire RNA replication complex (10, 12, 16, 44, 45, 47–50). Poliovirus 3A protein, for example, localizes to ER membranes when expressed in isolation (12, 15), and its precursor, 3AB, behaves as an integral membrane protein when translated in vitro in the presence of microsomal membranes, displaying resistance to extraction with high-salt, high-pH, and chaotropic agents (50).

Within infected cells, 3A-containing polypeptides are likely to play numerous roles. Some mutations in the 3A coding region give rise to viruses defective in RNA synthesis (6, 17, 18, 48, 49, 52, 53); certain substitutions for either Thr67 or Met79 give rise to viruses that are specifically defective in positive-strand synthesis (18, 48). Another mutation, 3A-2 (Fig. 1A), inserts an additional serine residue between amino acids 14 and 15 in the 3A coding sequence and gives rise to virus that does not inhibit cellular protein secretion as effectively as wild-type virus (6, 13–15). The I46T mutation in 3A has been reported to cause a host-specific defect in cell lysis (27). Such genetic analyses, however, cannot reveal whether the affected protein is the 3A product itself or a larger precursor, such as 3AB.

Biochemically, the 87-amino-acid poliovirus protein 3A has been shown to inhibit ER-to-Golgi traffic (16, 32); this ability is very sensitive to mutations, such as the 3A-2 mutation, in the amino-terminal sequences of the protein (15). Protein 3A expression was also shown to increase membrane permeability in both yeast and *Escherichia coli* cells (1, 25). Viral protein 3AB, on the other hand, has been shown to display several different biochemical properties, including direct binding to the viral-RNA-dependent RNA polymerase 3D (22, 30, 52–54), stimulation of 3D polymerase activity (26, 33, 36, 37), and stimulation of the protease activity of 3CD (26, 54). Given these disparate functions within infected cells, it was of interest to us to determine the precise membrane topology of the 3A coding sequences, especially the amino-terminal sequences required for the inhibition of host protein secretion, and to determine whether this topology was shared by the various 3A-containing polypeptides.

The possibility that portions of the membrane-associated proteins in the poliovirus RNA replication complex reside within the lumens of intracellular membranes on which RNA synthesis occurs was suggested by several observations. First, the amino terminus of 3A protein contains a putative glycosylation site that was shown to be glycosylated during in vitro translations in the presence of canine microsomes (12). In addition, the formation of double-membraned vesicles during poliovirus infection, which can be mimicked by the expression of viral proteins 2BC and 3A in isolation (44, 45), is likely to require some mechanism to juxtapose the luminal faces of the double membranes formed. Finally, for yellow fever virus, another positive-strand RNA virus, it has been shown that one of the nonstructural proteins, NS1, is required for RNA synthesis and is located exclusively within the lumens of the membranes

* Corresponding author. Mailing address: 299 Campus Dr., Stanford University School of Medicine, Stanford, CA 94305. Phone: (650) 498-7075. Fax: (650) 498-7147. karlak@leland.stanford.edu.

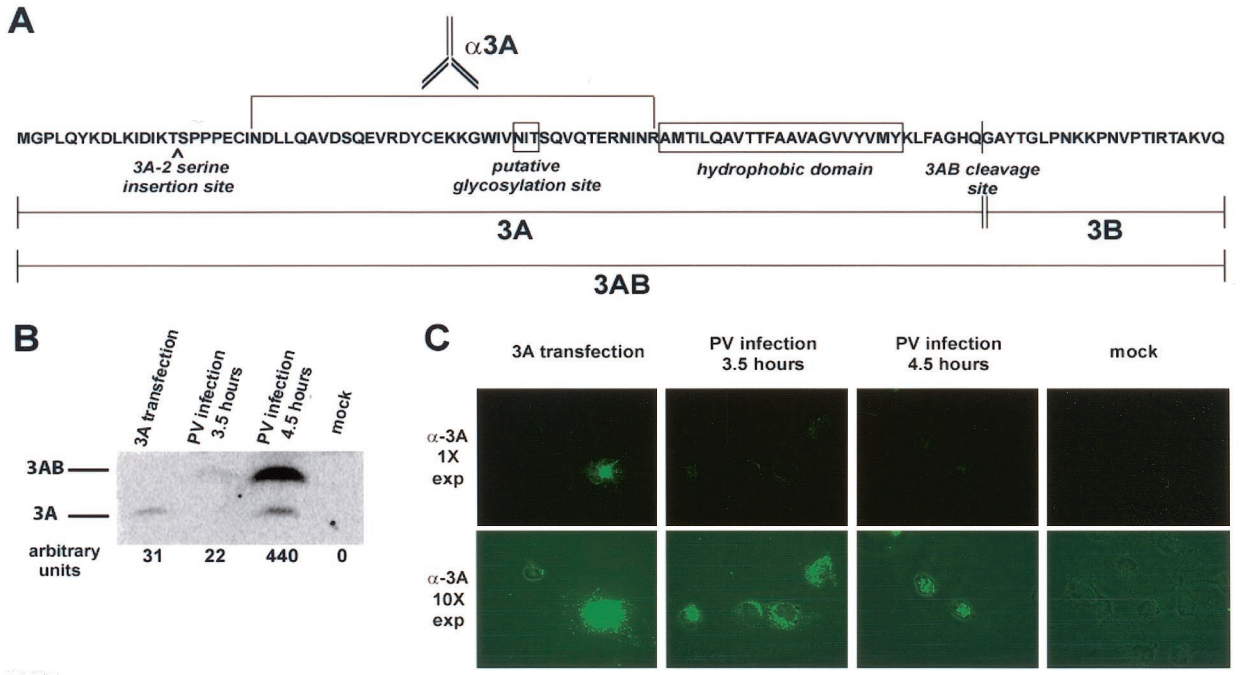

FIG. 1. Expression of 3A protein in transfected and infected COS cells. COS cells were plated onto coverslips and either transfected with a plasmid encoding 3A or infected with poliovirus at an MOI of 20 PFU/cell for the indicated amounts of time. The transfections and infections were performed in duplicate, and cells were processed for either indirect immunofluorescence or Western blot analysis. (A) PV 3AB amino acid sequence, with vertical bars denoting the N and C termini of 3A and 3B. (B) Western blot of cells expressing 3A from transfection or infection. Protein bands were developed on a PhosphorImager and quantified with ImageQuant software. (C) COS cells were fixed with 4% paraformaldehyde, permeabilized in 0.5 μg of digitonin per ml, and visualized with 3A monoclonal antibody followed by FITC-conjugated secondary antibody. Images obtained at 1× and 10× exposure times are shown. Fluorescence images have been overlaid with phase images in all panels.

on which the yellow fever virus RNA replication complex is assembled (28).

Previous experiments by Takegami et al. (46) showed that the amino terminus of poliovirus protein 3AB was accessible to digestion with trypsin. However, one could not conclude from these data that the amino-terminal sequences of the 3A protein were cytosolic, because an anti-3B antibody was used to probe the integrity of the proteins. Furthermore, no tests were performed to ensure that membrane topology was preserved during the extract preparation (46). Curiously, during expression studies of poliovirus protein 3A in the context of poliovirus infection and in isolation, we noticed a distinct lack of immunofluorescence using antibodies directed against 3A in virus-infected cells. This finding could indicate that the amino terminus of 3A itself was luminal and therefore inaccessible to antibody during the cell permeabilization protocols used. This hypothesis was tested here by both immunofluorescence and proteolytic digestion. Another possibility, that formation of the poliovirus RNA replication complex causes shielding of 3A epitopes, was investigated by comparing the immunofluorescence of 3A-containing proteins during wild-type-poliovirus infection and infection with a mutant poliovirus, M394T, that encodes a temperature-sensitive mutant RNA-dependent RNA polymerase with a defect near its 3AB-binding site (4). The results presented here support the hypothesis that the interaction between 3A-containing proteins and 3D polymerase during the formation of the replication complex is involved in shielding of 3A epitopes.

MATERIALS AND METHODS

Cells and viruses. COS-1 cells were cultured as monolayers in Dulbecco's modified Eagle medium supplemented with 10% (vol/vol) calf serum, 100 U of penicillin per ml, and 100 U of streptomycin per ml at 37°C and 5% CO_2. Wild-type and M394T mutant poliovirus type 1 Mahoney stocks were prepared in HeLa cells as described elsewhere (4, 23). Viral titers were determined by plaque assays on COS-1 cells as described elsewhere (16). All infections were performed in 6- or 10-cm tissue culture dishes containing 3.5×10^5 or 1×10^6 COS-1 cells, respectively, at a multiplicity of infection (MOI) of 20 PFU/cell for 4.5 h at 37°C, unless otherwise indicated.

Plasmids and transfections. The GFP–HO-2 plasmid construct was a generous gift from Tom A. Rapoport (Harvard University) (38). Briefly, it consists of the coding region of the green fluorescent protein (GFP) gene fused to the 5′ end of the coding region of the heme oxygenase 2 (HO-2) gene, under the transcriptional control of the cytomegalovirus promoter. The p5NC-α6-based DNA plasmid constructs used to express wild-type 3A and 3A-2 mutant protein under the transcriptional control of the simian virus 40 late promoter have been described (15). COS-1 cells were transfected in 10-cm tissue culture dishes by using Lipofectamine Plus reagents as described by the manufacturer, with 20 μl of Plus reagent and 30 μl of Lipofectamine reagent (Invitrogen Life Technologies, Carlsbad, Calif.). Either GFP–HO-2 plasmids (4 μg per transfection) or p5NC-α6-based plasmids (8 μg per transfection) were used for transfections. Cells were processed for either proteolysis or immunofluorescence 24 h following transfection.

Antibodies and reagents. Anti-Grp94 monoclonal rat antibody was purchased from Stressgen Biotechnologies Corp. (Victoria, British Columbia, Canada) and used at a dilution of 1:50 for immunofluorescence and 1:200 for immunoblot analysis. Anti-GFP monoclonal mouse antibody was purchased from Clontech (Palo Alto, Calif.) and used at a dilution of 1:1,000 for immunoblot analysis. Anti-3A monoclonal mouse antibody was a hybridoma supernatant (15) used at a dilution of 1:30 for immunofluorescence and 1:50 for immunoblot analysis. Anti-mouse alkaline phosphatase (AP)-conjugated secondary antibody was purchased from Jackson ImmunoResearch Laboratories, Inc. (West Grove, Pa.),

and used at a dilution of 1:10,000 for immunoblot analysis. Anti-rat AP-conjugated secondary antibody was purchased from Stressgen Biotechnologies Corp. and used at a dilution of 1:20,000 for immunoblot analysis. Fluorescein isothiocyanate (FITC)- and Texas Red-conjugated anti-mouse secondary antibodies were purchased from Vector Laboratories, Inc. (Burlingame, Calif.) and used at a dilution of 1:1,000 for immunofluorescence analysis. Prestained molecular weight markers and ECF reagent for the quantitative detection of AP-conjugated secondary antibodies were purchased from Amersham (Sunnyvale, Calif.). Digitonin and Triton X-100 were purchased from Sigma (St. Louis, Mo.). All reagents and antibodies were used and stored according to the manufacturer's suggestions.

Indirect immunofluorescence microscopy. COS-1 cells were plated onto coverslips in 6- or 10-cm tissue culture dishes 24 h before transfection. Twenty-four hours posttransfection, cells were washed three times with phosphate-buffered saline (PBS), fixed with 4% formaldehyde in PBS for 10 min at room temperature, washed three more times with PBS, and permeabilized with either 0.5% Triton X-100 (Sigma) in PBS for 10 min at room temperature or 0.5 μg of digitonin per ml in buffer D (0.3 M sucrose, 2.5 mM $MgCl_2$, 0.1 M KCl, 1 mM EDTA, and 10 mM PIPES; pH 6.8) for 5 min on ice. Following permeabilization, cells were incubated in PBS containing 1% bovine serum albumin (BSA) for 30 min at room temperature, incubated in the appropriate primary antibody in PBS–1% BSA for 1 h at room temperature, washed three times for 15 min in PBS–1% BSA, incubated with the appropriate secondary antibody in PBS–1% BSA for 1 h at room temperature, and washed again in PBS three times for 15 min each time. The coverslips were mounted on slides by using 5 to 10 μl of Vectashield (Vector Laboratories, Inc.) as an antifading agent. The slides were viewed on an upright fluorescent microscope equipped with a 40× objective and photographed by using a digital camera and ImagePro software (Media Cybernetics, Silver Spring, Md.). Quantitation of fluorescence intensities was performed using Metamorph software (Universal Imaging Corporation, Downingtown, Pa.).

Protease assay. For each proteolysis experiment, four 10-cm tissue culture dishes of COS-1 cells were transfected with GFP–HO-2 plasmid and then infected with poliovirus 24 h later for various times. Cells were harvested by the semipermeabilized-cell method of Pind et al. (35). Briefly, cells were washed three times with ice-cold 50/90 H/KOAc buffer (50 mM HEPES adjusted to pH 7.2 with KOH and 90 mM potassium acetate) and hypotonically swollen in 10/18 H/KOAc buffer (10 mM HEPES adjusted to pH 7.2 with KOH and 18 mM potassium acetate) for 10 min on ice. The hypotonic buffer was then aspirated, and the cells were scraped into 1 ml of ice-cold 50/90 H/KOAc buffer. Then 4 ml of scraped cells was added to 8 ml of ice-cold 50/90 H/KOAc buffer and collected by centrifugation at 800 × g for 4 min at 4°C to remove soluble cytosolic proteins. The cells were then resuspended in 2 ml of ice-cold PBS, split into two microcentrifuge tubes, and collected by centrifugation at 4°C for 4 min at 800 × g. The cell pellet in one tube was resuspended in ice-cold PBS and the other tube was resuspended in ice-cold PBS containing 0.5% Triton X-100 (Sigma). Both tubes were placed on a rotator at 4°C for 10 min; 100-μl aliquots were incubated with various concentrations of proteinase K (Sigma) for 15 min at 37°C. Proteolysis was stopped by the addition of 20 μl of a solution containing 1 mM phenylmethylsulfonyl fluoride (Sigma) and sodium dodecyl sulfate-polyacrylamide gel electrophoresis (SDS-PAGE) sample buffer. Samples were incubated at 100°C for 5 min, and 35 μl of each sample was loaded onto each of three SDS-PAGE gels.

SDS-PAGE gels and Western blotting. To analyze samples for 3AB and 3A, lysates were electrophoresed on a 16.5% Tricine–SDS gel (40). To analyze samples for Grp94 or GFP–HO-2, lysates were electrophoresed on an 8% glycine–SDS-PAGE gel (24). Following SDS-PAGE, samples were transferred to polyvinylidene difluoride membranes (Millipore, Billerica, Mass.) for 1 h at 800 mA, using a Hoefer tank transfer system (Hoefer Pharmacia Biotech, San Francisco, Calif.). The efficiency of transfer was verified by using prestained molecular weight markers (Amersham). After transfer was complete, membranes were blocked by rocking in PBS-T (PBS that contained 0.1% [vol/vol] Tween-20 [Sigma]) and 5% (wt/vol) Carnation nonfat dry milk for 1 h at room temperature. Membranes were rocked for 1 h at room temperature with the appropriate primary antibody diluted in PBS-T. Membranes were then washed four times in PBS-T for 10 min each time, rocked for 1 h at room temperature with the appropriate AP-conjugated secondary antibody, diluted in PBS-T, washed four times in PBS-T for 10 min each time, developed in ECF reagent (Amersham) for 5 min, viewed on a PhosphorImager (Molecular Dynamics, Sunnyvale, Calif.), and analyzed with ImageQuant software.

Molecular modeling. Modeling was performed with the Swiss PDB Viewer (http://www.expasy.ch/spdbv) (20), and rendered with POV-RAY (http://www.povray.org). Coordinates for the unit cell of the three-dimensional structure of poliovirus RNA-dependent RNA polymerase (21) were provided by J. Hansen (Yale University) and S. Schultz (Diné College) and can be obtained from the National Center for Biotechnology Information library under PDB identification number 1RDR.

RESULTS

Immunofluorescence of 3A protein in transfected and infected cells. During studies of the effects of poliovirus infection and the expression of poliovirus 3A protein in isolation, we compared the amounts of accumulated protein and the immunofluorescence signals observed from 3A-containing polypeptides using a monoclonal antibody that recognizes an epitope between amino acids 23 and 59 (Fig. 1A) (15). As shown by the immunoblot in Fig. 1B, less 3A protein accumulated in COS-1 cells transfected with the 3A-expressing plasmid than in cells that underwent 4.5 h of poliovirus infection. To determine the average amount of 3A in each cell, the difference between the transfection efficiency (30%) and the infection efficiency (100%) was taken into account. Nonetheless, it was striking to observe that the immunofluorescence signal obtained from transfected cells was much stronger than that from the infected cells, even at 4.5 h postinfection, when approximately 10-fold more 3A-containing proteins were present per cell in the infected population (Fig. 1C). Furthermore, no increase in fluorescent signal was observed between 3.5 and 4.5 h of poliovirus infection, although the amount of 3A and 3AB proteins increased 20-fold.

Two distinct hypotheses could account for the reduced immunofluorescence signal from poliovirus-infected cells compared to that from cells that expressed 3A protein in isolation. First, since permeabilization was performed with digitonin, which is known to permeabilize plasma but not intracellular membranes, it was possible that the amino-terminal epitope of 3A protein and its precursors was found within the lumen of an intracellular compartment in infected, but not transfected, cells. A second possibility was that the N terminus of 3A is cytosolic in both transfected and infected cells, but in infected cells the epitope is blocked from interacting with the monoclonal antibody. To distinguish between these possibilities, we tested the membrane topology of poliovirus 3A protein by protease digestion and immunofluorescence analysis under conditions in which the integrity of intracellular membranes was demonstrated.

Immunofluorescence analysis of 3A- and 3A-2-transfected COS cells. To test whether the N-terminal sequences of 3A protein were cytosolic in cells that expressed 3A in isolation, COS cells were transfected with a plasmid that encoded either wild-type 3A protein or 3A-2 protein, a mutant version of 3A that displays a reduced ability to disrupt ER-to-Golgi traffic (15). After 24 h, the cells were fixed and treated with either Triton X-100, to permeabilize both plasma and intracellular membranes, or with digitonin, to leave the intracellular membranes intact. As a control for the integrity of intracellular membrane topology, the immunofluorescence signal obtained from Grp94, known to reside within the lumen of the ER, was also tested. As shown in Fig. 2, Grp94 staining was readily detected in the Triton X-100-permeabilized, but not the digitonin-permeabilized, samples, arguing that the topology of the membranes was undisturbed during sample preparation. The immunofluorescence signal obtained using the anti-3A anti-

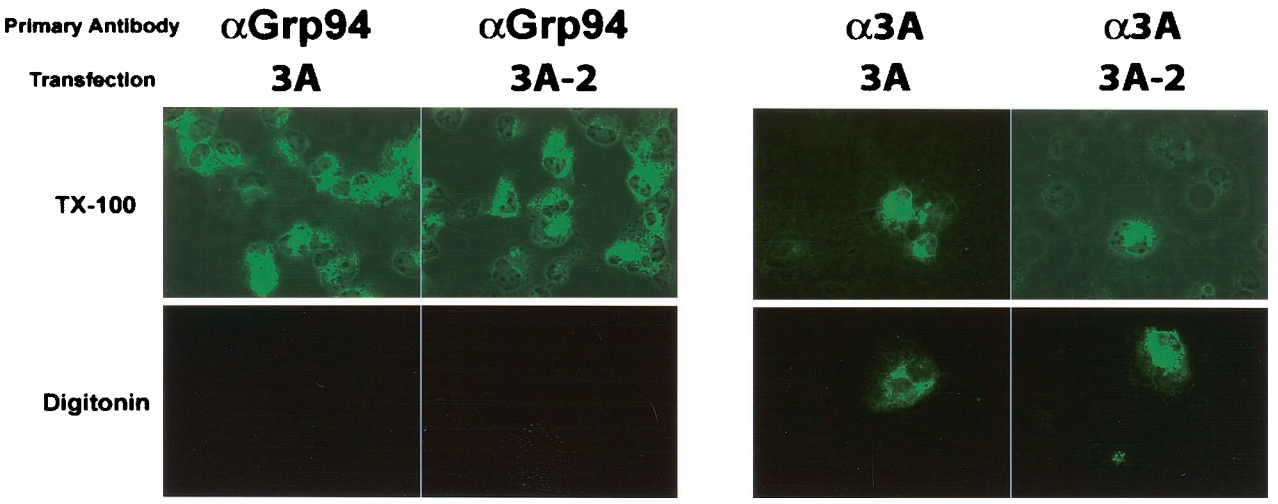

FIG. 2. Immunofluorescence of 3A- and 3A-2-transfected COS cells. COS cells were plated onto coverslips and transfected with the indicated construct. Cells were incubated at 37°C for 24 h and fixed in 4% paraformaldehyde. Selective permeabilization of the plasma membrane was performed in 0.5 μg of digitonin per ml. Permeabilization of all cellular membranes was performed in 0.5% Triton X-100 (TX-100). Immunofluorescence signal from 3A-containing proteins was visualized as described for Fig. 1. Fluorescence images have been overlaid with phase images in all panels.

body, on the other hand, was visible despite the method of permeabilization, supporting the hypothesis that at least part of the population of 3A proteins was exposed to the cytosol.

When expressed in isolation, poliovirus 3A protein inhibits host protein traffic from the ER to the Golgi apparatus at a step that has not yet been identified (13–15). The 3A-2 mutation reduces the ability of 3A protein in isolation, or of viruses that contain the mutation, to inhibit ER-to-Golgi traffic, but does not substantially interfere with viral growth (6, 14, 15). As shown in Fig. 2, 3A protein that contains the 3A-2 mutation also displayed cytosolic localization of its amino-terminal residues.

Immunofluorescence analysis of poliovirus-infected cells. During poliovirus infection, 3A protein sequences are found both in precursors such as 3AB and in the processed 3A product. To test whether the amino-terminal domains of 3A and larger 3A-containing proteins are localized on the cytosolic surface of membranes during poliovirus infection, and to test whether the N terminus of 3A is cytosolic during infection as it is following transfection, we performed immunofluorescence

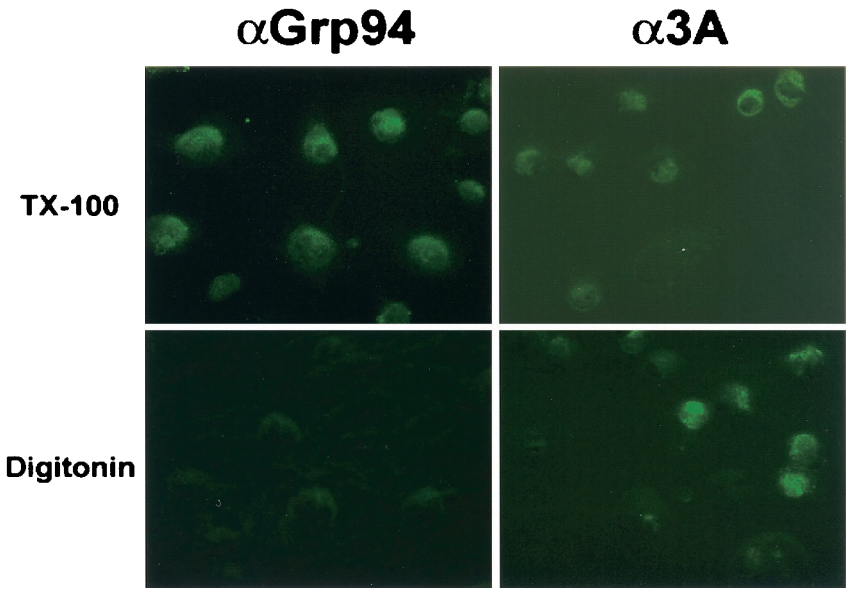

FIG. 3. Immunofluorescence of poliovirus-infected COS cells. COS cells were plated onto coverslips and infected with poliovirus at an MOI of 20 PFU/cell. Cells were then incubated at 37°C for 4.5 h and fixed in 4% paraformaldehyde. Selective permeabilization of the plasma membrane was performed in 0.5 μg of digitonin per ml. Permeabilization of all cellular membranes was performed in 0.5% Triton X-100 (TX-100). Fluorescence images have been overlaid with phase images in all panels.

analysis on poliovirus-infected cells. Grp94 staining of poliovirus-infected cells could be observed following Triton X-100 but not digitonin permeabilization, arguing that intracellular membranes were intact. However, the immunofluorescence signal obtained with anti-3A antibody did not depend on the permeabilization detergent used, arguing that 3A epitopes were exposed to the cytosol, as shown in Fig. 3.

Proteolytic digestion of 3A protein. Although the immunofluorescence analysis showed that some proportion of the 3A-containing proteins display cytosolic localization of their amino-terminal sequences, such analysis could not reveal the potential presence of a luminal subpopulation if there were heterogeneity in the topology of the protein or its precursors. To test the potential existence of a luminal subpopulation of 3A-containing proteins, we performed limited proteolysis on semipermeabilized cells. The plasma membranes of transfected and infected cells were mechanically permeabilized by hypotonic swelling, followed by scraping of the cells from the tissue culture dish. This technique lyses the cells while leaving the ER membranes intact, in the proper orientation, and functional to support anterograde transport (2, 5, 35). Semipermeabilized cells were washed to remove cytosolic contents and subjected to digestion with various concentrations of proteinase K in the absence or presence of Triton X-100. The degree of proteolysis of control and experimental proteins was determined by immunoblot analysis.

To determine the efficiency of plasma membrane lysis and the integrity of the ER, the luminal protein Grp94 and the fusion protein GFP–HO-2 (38) were monitored. As shown in Fig. 4A and D, the luminal ER protein Grp94 was susceptible to proteinase K in the presence, but not in the absence, of detergent, arguing that the ER remained intact during the permeabilization procedure. The cytosolic GFP–HO-2 protein, on the other hand, was 80% digested in the absence of detergent and 100% digested in the presence of detergent. The simplest explanation of this result is that the gentle technique used to render the cells semipermeable resulted in the lysis of only 80% of the cells.

During poliovirus infection, the patterns of proteolytic digestion of 3A and 3AB were identical to each other and to that of the cytosolic marker GFP–HO-2 (Fig. 4B to F). Specifically, in the absence of detergent, approximately 80% of 3A and 3AB were digested, consistent with the hypothesis that there is no protected subpopulation of either 3A or 3AB in produc-

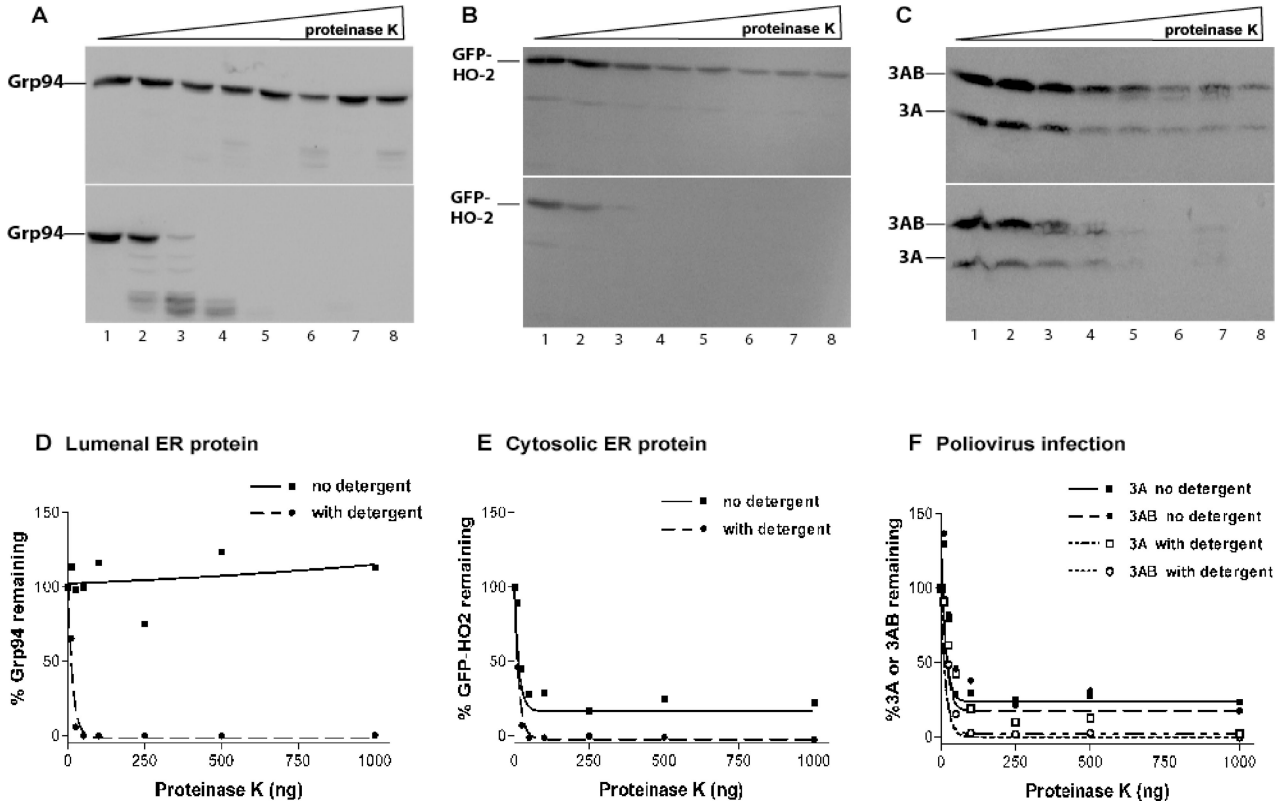

FIG. 4. Proteinase K digests of poliovirus-infected COS cells. COS cells were infected with poliovirus at an MOI of 20 PFU/cell and incubated for 4.5 h at 37°C. Cells were harvested for proteolysis by hypotonically swelling and scraping the cells from the tissue culture dish to selectively permeabilize the plasma membrane. Cells were washed to remove endogenous cytosolic components and resuspended in PBS in the absence (top portions of panels A to C) or presence (bottom portions of panels A to C) of 0.5% Triton X-100. Cells were incubated with increasing amounts of proteinase K (A to C: lane 1, 0 ng; lane 2, 10 ng; lane 3, 25 ng; lane 4, 50 ng; lane 5, 100 ng; lane 6, 250 ng; lane 7, 500 ng; lane 8, 1,000 ng) for 15 min at 37°C. Proteolysis was stopped by adding phenylmethylsulfonyl fluoride and sample buffer containing dithiothreitol and β-mercaptoethanol, followed by boiling for 5 min. Samples were run on SDS-PAGE gels, transferred to polyvinylidene difluoride membranes, probed with the indicated antibodies, and developed on a PhosphorImager to determine protease susceptibility. Proteinase K digests of Grp94 (A), a luminal ER marker, GFP–HO-2 (B), a cytosolic ER marker, and 3AB and 3A (C) are shown. Quantitation and graphing (D to F) were performed with ImageQuant and GraphPad Prism software.

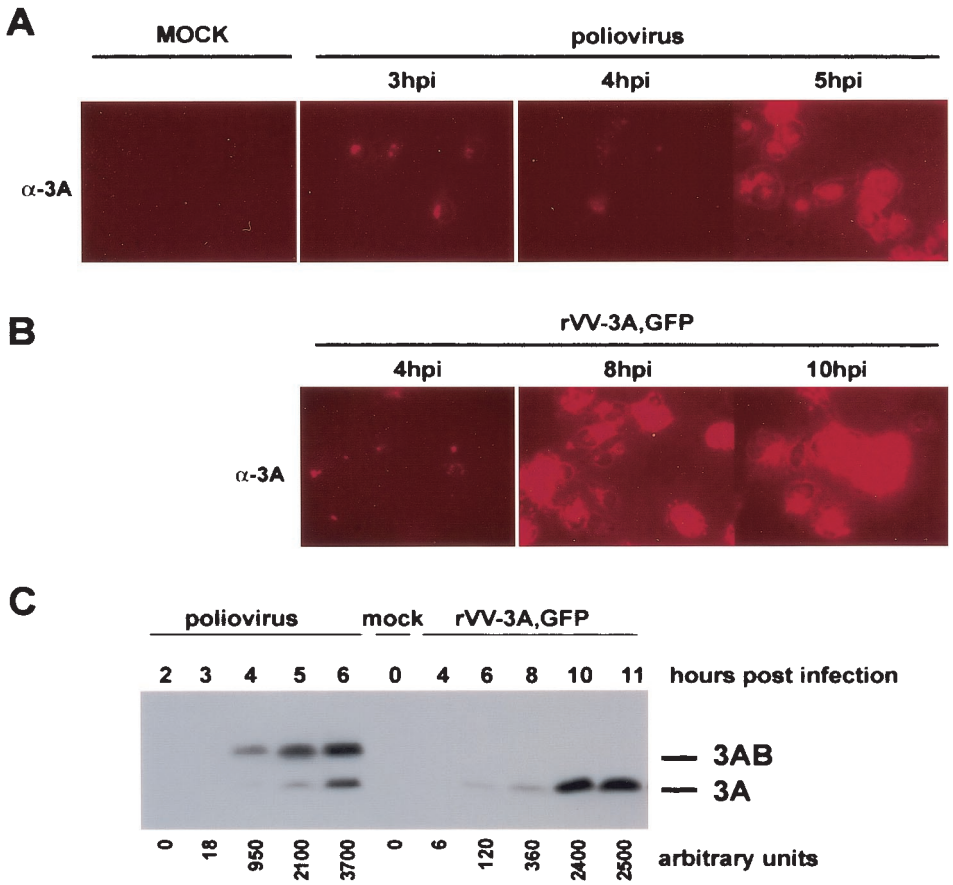

FIG. 5. Analysis of 3A protein during poliovirus and rVV-3A,GFP infection. COS cells were plated onto coverslips and mock infected or infected with either poliovirus or recombinant vaccinia virus, expressing 3A protein (rVV-3A,GFP), at an MOI of 20 PFU/cell and incubated at 37°C for the indicated amounts of time. All infections were performed in duplicate, and cells were processed for either indirect immunofluorescence or Western blot analysis. (A and B) COS cells were fixed with 4% paraformaldehyde, permeabilized in 0.5 μg of digitonin per ml, and stained with 3A monoclonal antibody followed by Texas Red-conjugated secondary antibody. Coverslips were mounted on slides with Vectashield and viewed on a fluorescent microscope with ImagePro software. Fluorescence images have been overlaid with phase images in all panels. (C) Western blot of 3AB and 3A expression during poliovirus or recombinant vaccinia virus infection over time. Protein bands were developed on a PhosphorImager and quantitated with ImageQuant software. The numbers below the lanes indicate relative intensities of the bands in each lane. Numbers for poliovirus infections are the sums of the 3AB and 3A bands.

tively infected cells (Fig. 4F). In the presence of detergent, as expected, 100% of the 3A and 3AB populations are susceptible to digestion with proteinase K. The results from these analyses are consistent with the results from the immunofluorescence analyses (Fig. 2), supporting the hypothesis that the amino termini of both 3AB and 3A are cytosolic. They also support the hypothesis that it is not the topology of 3AB or 3A but rather another factor that decreases the intensity of the 3AB or 3A immunofluorescence signal in infected cells.

Epitope shielding of 3A protein in wild-type poliovirus-infected but not vaccinia virus-infected cells. To test whether 3A-containing sequences are relatively inaccessible to antibody probes when present in a poliovirus RNA replication complex, we expressed poliovirus 3A in the context of vaccinia virus infection as well as during poliovirus infection (13). A vaccinia virus vector was chosen because, as with poliovirus infection, almost all of the cells on a tissue-culture plate could be infected in a uniform way, making it more straightforward to use immunoblot analysis to compare the amounts of 3A-containing proteins made in each cell under the two different conditions. As shown in Fig. 5, although no 3A-containing proteins were detectable by immunoblotting at 3 h after infection with poliovirus or 4 h after infection with rVV-3A,GFP virus, equivalent immunofluorescence signals were seen with the anti-3A antibody at both time points. However, by 4 h after infection with poliovirus, both 3AB and 3A were detectable by immunoblotting, giving an amount of 3A-containing proteins greater than that seen by 8 h after infection with rVV-3A,GFP. Nonetheless, the immunofluorescence signal seen in the poliovirus-infected cells was much reduced relative to that in the VV-3A-infected cells. At later time points, such as 5 h after infection with poliovirus, the shielding of the 3A immunofluorescence signal was not so pronounced (Fig. 5A). Therefore, 3A-containing polypeptides, definitely 3AB and probably 3A as well, are shielded from probing with antibodies by an intracellular process, concurrent with the formation of the poliovirus RNA replication complex, which forms between 3 and 4 h postinfection.

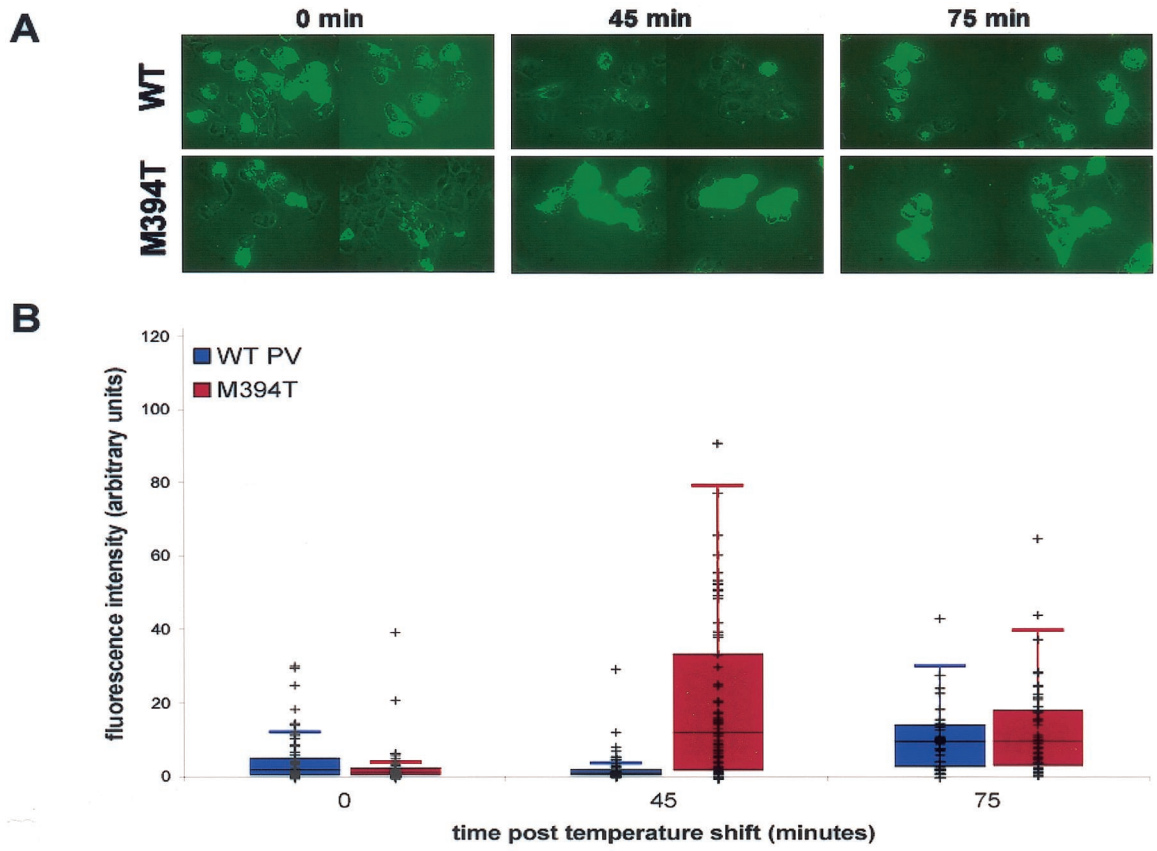

FIG. 6. Immunofluorescence of 3A protein during wild-type and 3D-M394T mutant poliovirus infection. COS cells were plated onto coverslips and infected at an MOI of 20 PFU/ml with either wild-type poliovirus or 3D-M394T, a temperature-sensitive mutant poliovirus (4). Infections were carried out at 32.5°C for 4 h, followed by the addition of 2 mM guanidine to inhibit RNA replication and further incubation at 39.5°C, the nonpermissive temperature for the M394T mutant virus, as indicated. All infections were performed in duplicate, and cells were processed for indirect immunofluorescence or immunoblot analysis. (A) COS cells were fixed, permeabilized in digitonin, and stained with 3A monoclonal antibody followed by FITC-conjugated secondary antibody. Fluorescence images have been overlaid with phase images in all panels. (B) Quantitation of the average fluorescence intensity per cell during either wild-type or M394T mutant poliovirus infection at the indicated times after the temperature shift. Fluorescence intensities of 35 to 70 cells per experiment were measured with Metamorph software (Universal Imaging Corporation). Data for each cell were plotted and overlaid onto a box plot of the first and third quartiles and the median, with error bars. Quartiles and box plots were made with R Lab 1 statistical analysis software (http://cran.r-project.org).

Immunofluorescence of 3A protein during wild-type and M394T mutant poliovirus infections. Poliovirus protein 3AB is known to bind directly to the viral RNA-dependent RNA polymerase, 3D (7, 8, 11, 31, 39, 41, 42, 44, 45), making 3D polymerase a likely candidate for the protein that directly shields the 3A epitope. A well-characterized mutant virus, 3D-M394T, contains a single mutation in the polymerase coding region, displays a temperature-sensitive RNA replication defect in infected cells, and shows a specific defect in the initiation of RNA replication in cell-free assays (4). Met394 in 3D polymerase is adjacent to the defined 3AB-binding site, and the purified M394T polymerase is defective in the addition of uridylyl residues to 3B (VPg), the protein primer for RNA synthesis (34). To test whether the 3A and 3AB epitope shielding observed during wild-type poliovirus infection would be less pronounced in the presence of a 3D polymerase potentially defective in these interactions, the immunofluorescence signals of 3A-containing proteins in wild-type and M394T infections were compared. Further incubation was continued at 39.5°C in the presence of 2 mM guanidine to inhibit RNA replication of the wild-type as well as the temperature-sensitive virus.

As shown in Fig. 6, the immunofluorescence signals at 0 and 75 min after the temperature shift were comparable between the wild-type and mutant viruses. However, the immunofluorescence signal of 3A during wild-type poliovirus infection at 45 min after the temperature shift was significantly less than during M394T mutant poliovirus infection. The difference in the signals was not due to a greater amount of 3A and 3AB proteins during wild-type poliovirus infection than during M394T mutant poliovirus infection, because immunoblot analysis demonstrated that 3A-containing proteins were more abundant during the wild-type infection than during the M394T infection (data not shown).

To quantify the fluorescence signal from 3A-containing proteins during wild-type and M394T mutant virus infection, the fluorescence intensities of 35 to 70 randomly chosen cells from each condition were measured. As can be seen in Fig. 6B, the temperature-sensitive virus showed substantially increased fluorescence, and therefore reduced epitope shielding, at the

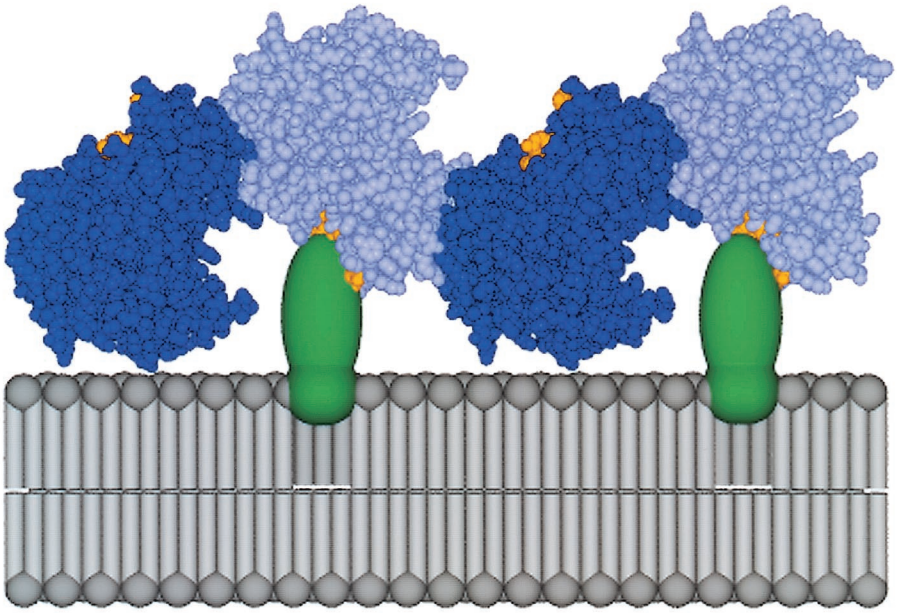

FIG. 7. Model of the oligomeric polymerase lattice bound to membrane-associated 3AB in a poliovirus-infected cell. A model for the mechanism of 3A epitope shielding, via the interaction between 3AB and a higher-order polymerase structure, is shown. 3AB is represented as a globular, integral membrane protein (green). 3D polymerase molecules, forming contacts along an interface observed in the three-dimensional structure interface I (21) are shown in dark blue and light blue. This view does not indicate a second interface, which may form between these fibers of polymerase molecules to give rise to two-dimensional lattices (29). The surface of 3D polymerase known to interact with 3AB through the 3AB binding site (22, 30) is shown in orange. Every second polymerase molecule could directly contact membrane-associated 3AB. Coordinates for the unit cell of the three-dimensional poliovirus RNA-dependent RNA polymerase (21) were provided by J. Hansen (Yale University) and S. Schultz (Diné College) and can be obtained from the National Center for Biotechnology Information library under PDB identification number 1RDR. This figure was kindly provided by Joanna Boerner (Stanford University).

nonpermissive temperature. Therefore, the increased signal from the M394T infection at the nonpermissive temperature was due to increased availability of 3A-containing proteins to antibody. Parenthetically, this was probably also the case at the "permissive" temperature for the M394T mutant virus. As can be seen in Fig. 6 at the 0-min point, the M394T mutant-infected cells yielded a fluorescent signal similar to that of the cells infected with wild-type virus, in which 3A-containing proteins were more abundant. The reduction in shielding caused by the M394T mutation in the viral polymerase was more dramatic, however, after the temperature shift.

DISCUSSION

Both 3A and 3AB proteins accumulate in poliovirus-infected cells and are known or suspected to play several roles during viral infection. Furthermore, there are likely to be additional, and currently unknown, functions carried out by larger, 3A precursor proteins. Therefore, it is important to investigate the conformation and topology of both the final digestion products and precursor proteins that accumulate during infection.

Viral protein 3AB is known to target to ER membranes within cells and to bind directly to the viral RNA-dependent RNA polymerase 3D (12, 16, 22, 25, 36, 50, 52). The 22-amino-acid 3B sequences serve as the primer for RNA synthesis (34), although it is not yet known whether they carry out this priming function in infected cells before or after cleavage from 3AB or some larger precursor (51).

Viral 3A sequences are likely to participate directly in the formation of the membranous vesicles on which RNA replication occurs. In infections with some other positive-strand RNA viruses, expression of a large precursor protein that comprises sequences homologous to 2B, 2C, and 3A is required to induce vesicle formation (9). Although poliovirus protein 2BC can, in isolation, cause the formation of membranous vesicles (3, 10), these vesicles change morphology when viral protein 3A is coexpressed to resemble more closely the vesicles induced during poliovirus infection (44, 45). The conversion of the single-membraned vesicles induced by 2BC protein into double-membraned vesicles during coexpression of 2BC and 3A makes it likely that 3A or a larger 3A-containing precursor causes or promotes contact between two ER-derived membranes, which might suggest a luminal function. It had been previously suggested that the amino-terminal sequences of at least a subset of 3A molecules might be luminal, due to the utilization in vitro of a putative N-terminal glycosylation site in 3A (12). Nonetheless, both the immunofluorescence and proteolytic processing data presented here argue that the amino-terminal domain of 3A is cytosolic both in infected cells and in cells that express 3A in isolation. Therefore, it is likely that all functions of 3A, including the inhibition of ER-to-Golgi traffic both during infection and in expression in isolation (15, 16, 32), are accomplished by using this topology.

Despite the similar intracellular topology, the intensity of the immunofluorescence signal observed with anti-3A antibodies was greater when 3A was expressed via transfection or a

vaccinia virus vector, compared to bona fide poliovirus infection. Immunoblot analysis revealed that the reduction in 3A immunofluorescence observed at 4 h postinfection was observed even when larger quantities of 3A-containing sequences were detected by immunoblot analysis (Fig. 1 and 5). This shielding was not observed at later time points (Fig. 5). On the other hand, during infection with 3D-M394T virus, a temperature-sensitive poliovirus that contains a mutation near the 3AB binding site on the polymerase, greater 3A fluorescence was observed after the temperature shift (Fig. 6). The decreased epitope shielding seen with temperature-sensitive mutant polymerase suggests that it is the interaction of 3A-containing proteins with 3CD or 3D that leads to the masking of the 3A epitope.

Shielding of specific epitopes has been found previously to correlate with protein conformational changes or higher-order interactions within cells. Examples include the inhibition of c-Myc function and epitope masking by the Tax protein of human T-cell leukemia virus type 1 (43) and the shielding of a specific actin epitope in myofibrils and stress fibers but not in nuclear actin-containing structures (19). During poliovirus infection, the 3A epitope found in the amino-terminal domain becomes shielded at approximately 4 h postinfection, the time at which RNA replication complexes are maximally active (Fig. 5). The shielded epitope in 3A lies within a paired α-helical region likely to be involved in 3A dimerization (44, 45). We do not yet know the physical basis for this epitope masking, although it is likely to be a conformational change in the 3A sequences or physical occlusion by the formation of a new complex associated with RNA replication.

One of the functions of poliovirus protein 3AB is to tether the soluble RNA-dependent RNA polymerase to the membranes on which RNA replication occurs (22, 26, 50, 52). The contact surface on the 3AB molecule has not been identified structurally, but two-hybrid analysis has suggested that many of these contacts are within 3B sequences (52). The contact surface on poliovirus 3D polymerase has been identified by alanine scanning (30) and lies in a hydrophobic patch near conserved motif E (21). A possible mechanism for the blocking of 3A epitopes by the binding of polymerase 3D, larger 3D-containing proteins such as 3CD, or both is provided by the observed oligomerization of 3D into two-dimensional lattices (29), modeled in Fig. 7. When the lattices are modeled by using contacts identified by the known crystal structure of 3D polymerase (21), half of the polymerase molecules in the lattice could directly contact membrane-associated 3AB (Fig. 7), suggesting a physical basis for the observed epitope masking that can be tested experimentally. The shielding of 3A epitopes concomitant with the formation of the poliovirus RNA replication complex may provide an additional tool to investigate the assembly of the complex within cells and its disruption by mutations and antiviral compounds.

ACKNOWLEDGMENTS

We thank our colleagues Peter Sarnow, Bill Jackson, and Julie Pfeiffer for comments on the manuscript. We gratefully acknowledge Joanna Boerner for helpful discussions and for the modeling of the 3AB-3D interaction, Andres Tellez for help with statistical analyses, Joshua Jones for assistance with quantitative immunofluorescence, and Kurt Gustin for helpful insights.

This work was supported by funding from the National Institutes of Health.

REFERENCES

1. **Aldabe, R., A. Barco, and L. Carrasco.** 1996. Membrane permeabilization by poliovirus proteins 2B and 2BC. J. Biol. Chem. **271:**23134–23137.
2. **Balch, W. E., K. R. Wagner, and D. S. Keller.** 1987. Reconstitution of transport of vesicular stomatitis virus G protein from the endoplasmic reticulum to the Golgi complex using a cell-free system. J. Cell Biol. **104:**749–760.
3. **Barco, A., and L. Carrasco.** 1995. A human virus protein, poliovirus protein 2BC, induces membrane proliferation and blocks the exocytic pathway in the yeast Saccharomyces cerevisiae. EMBO J. **14:**3349–3364.
4. **Barton, D. J., B. J. Morasco, L. Eisner-Smerage, P. S. Collis, S. E. Diamond, M. J. Hewlett, M. A. Merchant, B. J. O'Donnell, and J. B. Flanegan.** 1996. Poliovirus RNA polymerase mutation 3D-M394T results in a temperature-sensitive defect in RNA synthesis. Virology **217:**459–469.
5. **Beckers, C. J., D. S. Keller, and W. E. Balch.** 1989. Preparation of semiintact Chinese hamster ovary cells for reconstitution of endoplasmic reticulum-to-Golgi transport in a cell-free system. Methods Cell Biol. **31:**91–102.
6. **Bernstein, H. D., and D. Baltimore.** 1988. Poliovirus mutant that contains a cold-sensitive defect in viral RNA synthesis. J. Virol. **62:**2922–2928.
7. **Bienz, K., D. Egger, and T. Pfister.** 1994. Characteristics of the poliovirus replication complex. Arch. Virol. Suppl. **9:**147–157.
8. **Bienz, K., D. Egger, T. Pfister, and M. Troxler.** 1992. Structural and functional characterization of the poliovirus replication complex. J. Virol. **66:** 2740–2747.
9. **Carette, J. E., J. van Lent, S. A. MacFarlane, J. Wellink, and A. van Kammen.** 2002. Cowpea mosaic virus 32- and 60-kilodalton replication proteins target and change the morphology of endoplasmic reticulum membranes. J. Virol. **76:**6293–6301.
10. **Cho, M. W., N. Teterina, D. Egger, K. Bienz, and E. Ehrenfeld.** 1994. Membrane rearrangement and vesicle induction by recombinant poliovirus 2C and 2BC in human cells. Virology **202:**129–145.
11. **Dales, S., H. J. Eggers, I. Tamm, and G. E. Palade.** 1965. Electron microscopic study of the formation of poliovirus. Virology **26:**379–389.
12. **Datta, U., and A. Dasgupta.** 1994. Expression and subcellular localization of poliovirus VPg-precursor protein 3AB in eukaryotic cells: evidence for glycosylation in vitro. J. Virol. **68:**4468–4477.
13. **Deitz, S. B., D. A. Dodd, S. Cooper, P. Parham, and K. Kirkegaard.** 2000. MHC I-dependent antigen presentation is inhibited by poliovirus protein 3A. Proc. Natl. Acad. Sci. USA **97:**13790–13795.
14. **Dodd, D. A., T. H. Giddings, Jr., and K. Kirkegaard.** 2001. Poliovirus 3A protein limits interleukin-6 (IL-6), IL-8, and beta interferon secretion during viral infection. J. Virol. **75:**8158–8165.
15. **Doedens, J. R., T. H. Giddings, Jr., and K. Kirkegaard.** 1997. Inhibition of endoplasmic reticulum-to-Golgi traffic by poliovirus protein 3A: genetic and ultrastructural analysis. J. Virol. **71:**9054–9064.
16. **Doedens, J. R., and K. Kirkegaard.** 1995. Inhibition of cellular protein secretion by poliovirus proteins 2B and 3A. EMBO J. **14:**894–907.
17. **Giachetti, C., S. S. Hwang, and B. L. Semler.** 1992. *cis*-acting lesions targeted to the hydrophobic domain of a poliovirus membrane protein involved in RNA replication. J. Virol. **66:**6045–6057.
18. **Giachetti, C., and B. L. Semler.** 1991. Role of a viral membrane polypeptide in strand-specific initiation of poliovirus RNA synthesis. J. Virol. **65:**2647–2654.
19. **Gonsior, S. M., S. Platz, S. Buchmeier, U. Scheer, B. M. Jockusch, and H. Hinssen.** 1999. Conformational difference between nuclear and cytoplasmic actin as detected by a monoclonal antibody. J. Cell Sci. **112**(Pt. 6)**:**797–809.
20. **Guex, N., and M. C. Peitsch.** 1997. SWISS-MODEL and the Swiss-PdbViewer: an environment for comparative protein modeling. Electrophoresis **18:**2714–2723.
21. **Hansen, J. L., A. M. Long, and S. C. Schultz.** 1997. Structure of the RNA-dependent RNA polymerase of poliovirus. Structure **5:**1109–1122.
22. **Hope, D. A., S. E. Diamond, and K. Kirkegaard.** 1997. Genetic dissection of interaction between poliovirus 3D polymerase and viral protein 3AB. J. Virol. **71:**9490–9498.
23. **Kirkegaard, K., and D. Baltimore.** 1986. The mechanism of RNA recombination in poliovirus. Cell **47:**433–443.
24. **Laemmli, U. K.** 1970. Cleavage of structural proteins during the assembly of the head of bacteriophage T4. Nature **227:**680–685.
25. **Lama, J., and L. Carrasco.** 1992. Expression of poliovirus nonstructural proteins in Escherichia coli cells. Modification of membrane permeability induced by 2B and 3A. J. Biol. Chem. **267:**15932–15937.
26. **Lama, J., A. V. Paul, K. S. Harris, and E. Wimmer.** 1994. Properties of purified recombinant poliovirus protein 3aB as substrate for viral proteinases and as co-factor for RNA polymerase 3Dpol. J. Biol. Chem. **269:**66–70.
27. **Lama, J., M. A. Sanz, and L. Carrasco.** 1998. Genetic analysis of poliovirus protein 3A: characterization of a non-cytopathic mutant virus defective in killing Vero cells. J. Gen. Virol. **79**(Pt. 8)**:**1911–1921.
28. **Lindenbach, B. D., and C. M. Rice.** 1999. Genetic interaction of flavivirus nonstructural proteins NS1 and NS4A as a determinant of replicase function. J. Virol. **73:**4611–4621.

29. **Lyle, J. M., E. Bullitt, K. Bienz, and K. Kirkegaard.** 2002. Visualization and functional analysis of RNA-dependent RNA polymerase lattices. Science **296:**2218–2222.
30. **Lyle, J. M., A. Clewell, K. Richmond, O. C. Richards, D. A. Hope, S. C. Schultz, and K. Kirkegaard.** 2002. Similar structural basis for membrane localization and protein priming by an RNA-dependent RNA polymerase. J. Biol. Chem. **277:**16324–16331.
31. **Mattern, C. F., and W. A. Daniel.** 1965. Replication of poliovirus in HeLa cells: electron microscopic observations. Virology **26:**646–663.
32. **Neznanov, N., A. Kondratova, K. M. Chumakov, B. Angres, B. Zhumabayeva, V. I. Agol, and A. V. Gudkov.** 2001. Poliovirus protein 3A inhibits tumor necrosis factor (TNF)-induced apoptosis by eliminating the TNF receptor from the cell surface. J. Virol. **75:**10409–10420.
33. **Paul, A. V., X. Cao, K. S. Harris, J. Lama, and E. Wimmer.** 1994. Studies with poliovirus polymerase 3Dpol. Stimulation of poly(U) synthesis in vitro by purified poliovirus protein 3AB. J. Biol. Chem. **269:**29173–29181.
34. **Paul, A. V., J. H. van Boom, D. Filippov, and E. Wimmer.** 1998. Protein-primed RNA synthesis by purified poliovirus RNA polymerase. Nature **393:** 280–284.
35. **Pind, S., H. Davidson, R. Schwaninger, C. J. Beckers, H. Plutner, S. L. Schmid, and W. E. Balch.** 1993. Preparation of semiintact cells for study of vesicular trafficking in vitro. Methods Enzymol. **221:**222–234.
36. **Plotch, S. J., and O. Palant.** 1995. Poliovirus protein 3AB forms a complex with and stimulates the activity of the viral RNA polymerase, 3Dpol. J. Virol. **69:**7169–7179.
37. **Richards, O. C., and E. Ehrenfeld.** 1998. Effects of poliovirus 3AB protein on 3D polymerase-catalyzed reaction. J. Biol. Chem. **273:**12832–12840.
38. **Rolls, M. M., P. A. Stein, S. S. Taylor, E. Ha, F. McKeon, and T. A. Rapoport.** 1999. A visual screen of a GFP-fusion library identifies a new type of nuclear envelope membrane protein. J. Cell Biol. **146:**29–44.
39. **Rust, R. C., L. Landmann, R. Gosert, B. L. Tang, W. Hong, H. P. Hauri, D. Egger, and K. Bienz.** 2001. Cellular COPII proteins are involved in production of the vesicles that form the poliovirus replication complex. J. Virol. **75:**9808–9818.
40. **Schagger, H., and G. von Jagow.** 1987. Tricine-sodium dodecyl sulfate-polyacrylamide gel electrophoresis for the separation of proteins in the range from 1 to 100 kDa. Anal. Biochem. **166:**368–379.
41. **Schlegel, A., and K. Kirkegaard.** 1995. Cell biology of enterovirus infection, p. 135–154. *In* H. A. Rotbart (ed.), Human enterovirus infections. American Society for Microbiology, Washington, D.C.
42. **Schlegel, A., T. H. Giddings, Jr., M. S. Ladinsky, and K. Kirkegaard.** 1996. Cellular origin and ultrastructure of membranes induced during poliovirus infection. J. Virol. **70:**6576–6588.
43. **Semmes, O. J., J. F. Barret, C. V. Dang, and K. T. Jeang.** 1996. Human T-cell leukemia virus type I tax masks c-Myc function through a cAMP-dependent pathway. J. Biol. Chem. **271:**9730–9738.
44. **Strauss, D. M., L. W. Glustrom, and D. S. Wuttke.** 2003. Towards an understanding of the poliovirus replication complex: the solution structure of the soluble domain of the poliovirus 3A protein. J. Mol. Biol. **330:**225–234.
45. **Suhy, D. A., T. H. Giddings, Jr., and K. Kirkegaard.** 2000. Remodeling the endoplasmic reticulum by poliovirus infection and by individual viral proteins: an autophagy-like origin for virus-induced vesicles. J. Virol. **74:**8953–8965.
46. **Takegami, T., B. L. Semler, C. W. Anderson, and E. Wimmer.** 1983. Membrane fractions active in poliovirus RNA replication contain VPg precursor polypeptides. Virology **128:**33–47.
47. **Teterina, N. L., A. E. Gorbalenya, D. Egger, K. Bienz, and E. Ehrenfeld.** 1997. Poliovirus 2C protein determinants of membrane binding and rearrangements in mammalian cells. J. Virol. **71:**8962–8972.
48. **Teterina, N. L., M. S. Rinaudo, and E. Ehrenfeld.** 2003. Strand-specific RNA synthesis defects in a poliovirus with a mutation in protein 3A. J. Virol. **77:**12679–12691.
49. **Towner, J. S., D. M. Brown, J. H. Nguyen, and B. L. Semler.** 2003. Functional conservation of the hydrophobic domain of polypeptide 3AB between human rhinovirus and poliovirus. Virology **314:**432–442.
50. **Towner, J. S., T. V. Ho, and B. L. Semler.** 1996. Determinants of membrane association for poliovirus protein 3AB. J. Biol. Chem. **271:**26810–26818.
51. **Towner, J. S., M. M. Mazanet, and B. L. Semler.** 1998. Rescue of defective poliovirus RNA replication by 3AB-containing precursor polyproteins. J. Virol. **72:**7191–7200.
52. **Xiang, W., A. Cuconati, D. Hope, K. Kirkegaard, and E. Wimmer.** 1998. Complete protein linkage map of poliovirus P3 proteins: interaction of polymerase 3Dpol with VPg and with genetic variants of 3AB. J. Virol. **72:**6732–6741.
53. **Xiang, W., A. Cuconati, A. V. Paul, X. Cao, and E. Wimmer.** 1995. Molecular dissection of the multifunctional poliovirus RNA-binding protein 3AB. RNA **1:**892–904.
54. **Xiang, W., K. S. Harris, L. Alexander, and E. Wimmer.** 1995. Interaction between the 5′-terminal cloverleaf and 3AB/3CDpro of poliovirus is essential for RNA replication. J. Virol. **69:**3658–3667.